Electronic Supplementary Information (ESI) for

Fabrication of paper strip for a facile and rapid detection of bovine viral diarrhea virus *via* signal enhancement by copper polyhedral nanoshell

Min Woo Kim[a†], Hong-Je Park[b,c†], Chan Yeong Park[a], Ji Hong Kim[d], Chae Hwan Cho[d], Le Minh Tu Phan[a], Jong Pil Park[d], Suresh Kumar Kailasa[e], Chi-Ho Lee[c*], Tae Jung Park[a*]

[a]*Department of Chemistry, Institute of Interdisciplinary Convergence Research, Research Institute of Chem-Bio Diagnostic Technology, Chung-Ang University, 84 Heukseok-ro, Dongjak-gu, Seoul 06974, Republic of Korea*

[b]*R&D Center, Medexx Co., Ltd, 5F, #B, Korea Bio Park, 700 Daewangpangyo-ro, Bundang-gu, Seongnam-si, Gyeonggi-do 13488, Republic of Korea*

[c]*Department of Food Science and Biotechnology of Animal Resources, Konkuk University, 120 Neungdong-ro, Gwangjin-gu, Seoul 05029, Republic of Korea*

[d]*Department of Food Science and Biotechnology, Chung-Ang University, Ansung 17546, Republic of Korea*

[e]*Department of Applied Chemistry, Sardar Vallabhbhai National Institute of Technology, Surat–395007, Gujarat, India*

[†]These authors contributed equally to this work.

*Corresponding authors.

E-mail address: leech@konkuk.ac.kr (C.-H. Lee); tjpark@cau.ac.kr (T.J. Park)

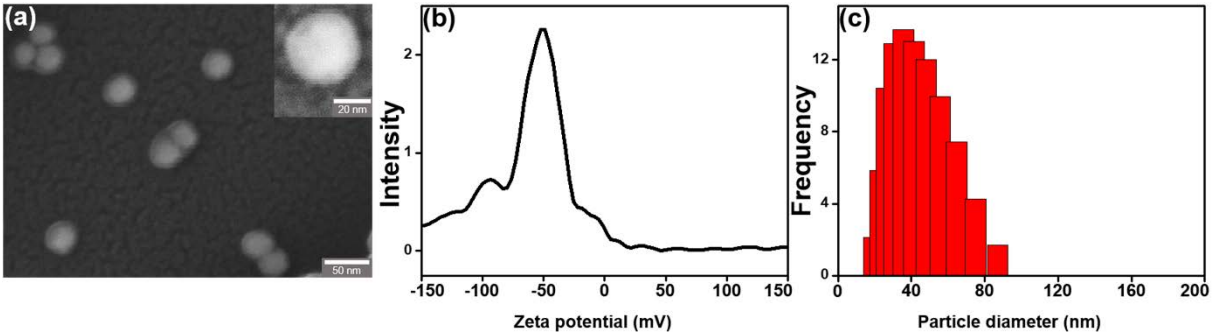

Fig. S1. (a) FE-SEM image of AuNPs well-dispersed with a narrow size distribution of 40 nm, which is well-matched with particle size analysis data (Scale bars represent 50 nm and 20 nm in an inset, respectively). (b) Zeta potential of AuNPs of –49.10 mV. (c) The size distribution of AuNPs by DLS analysis. The average diameter shows approximately 40 nm.

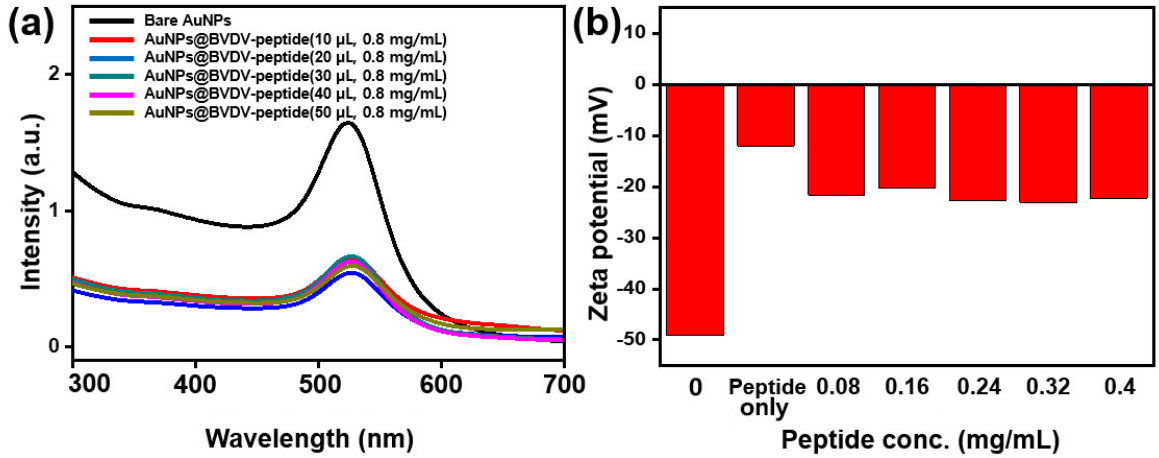

Fig. S2. Optimization of BVDV peptide concentration to conjugate on the AuNPs surface. (a) Absorption spectra of AuNPs and different concentrations of BVDV peptide. (b) Zeta potential of different concentrations of BVDV peptide conjugated onto the bare surface of AuNPs. Peptide only represents free peptide of 0.24 mg/mL without AuNPs.

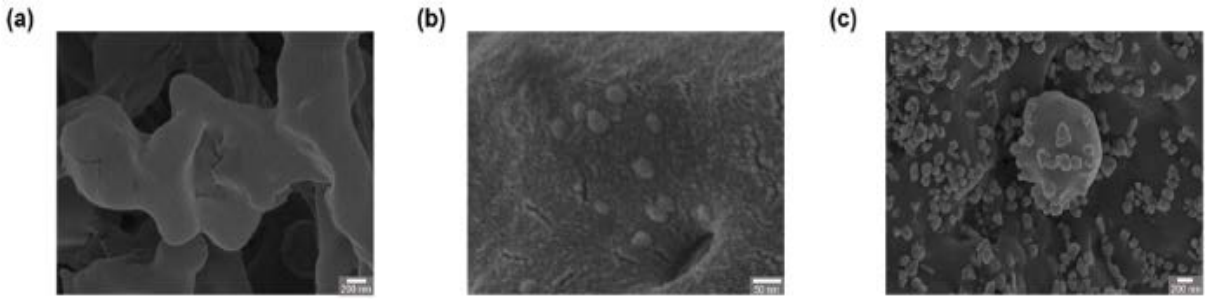

Fig. S3. FE-SEM images of (a) bare nitrocellulose (NC) membrane, (b) BVDV-peptide-AuNPs modified on the NC membrane, and (c) Cu and polyethyleneimine (PEI)-covered growth by highly specific CuP growth around the AuNPs on the NC membrane surface. The scale bars represent 200 nm, 50 nm, and 200 nm, respectively.

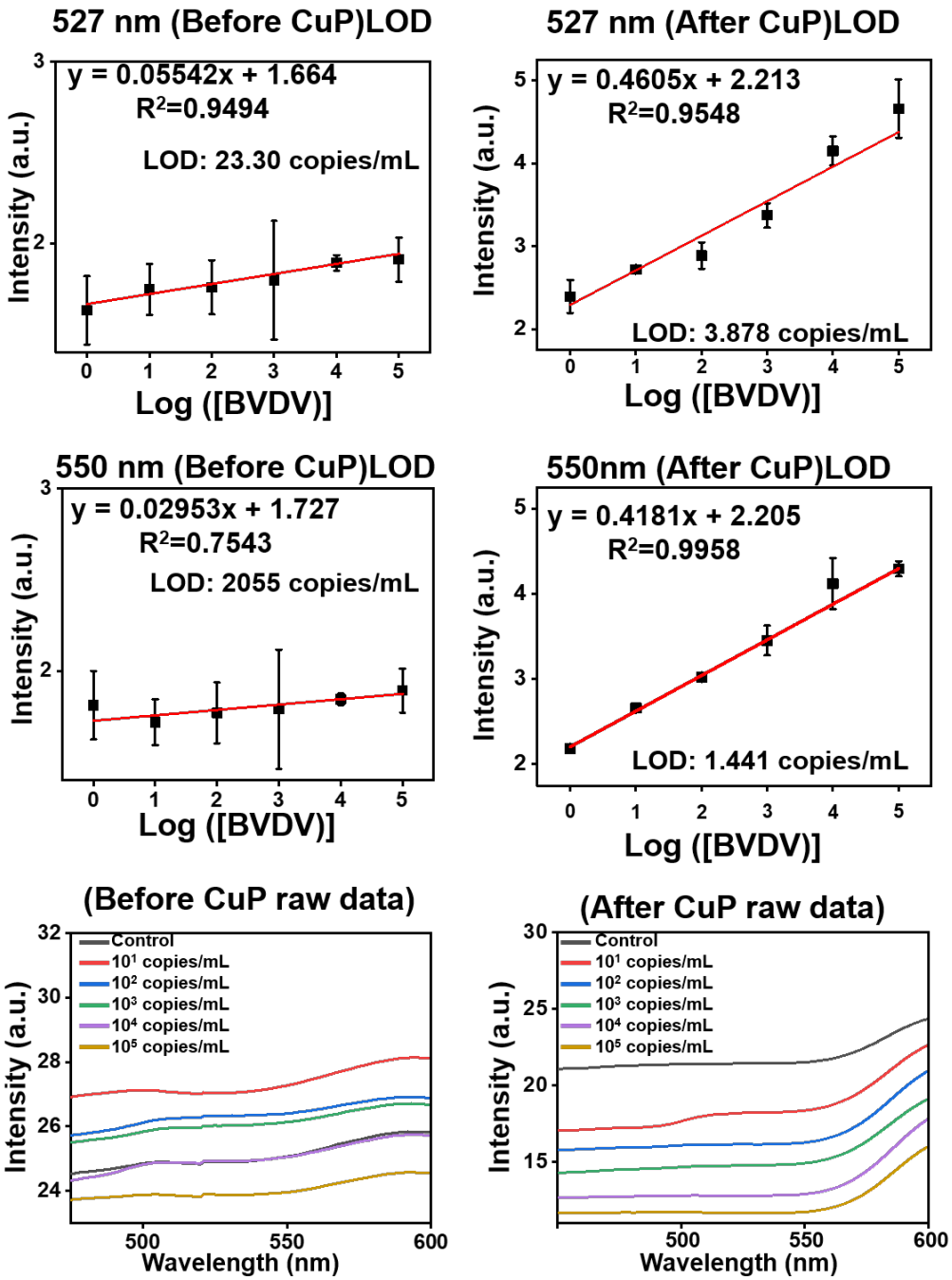

Fig. S4. Comparison of the signal intensities at different wavelengths (527 nm and 550 nm) before CuP treatment (left) and after CuP treatment (right).

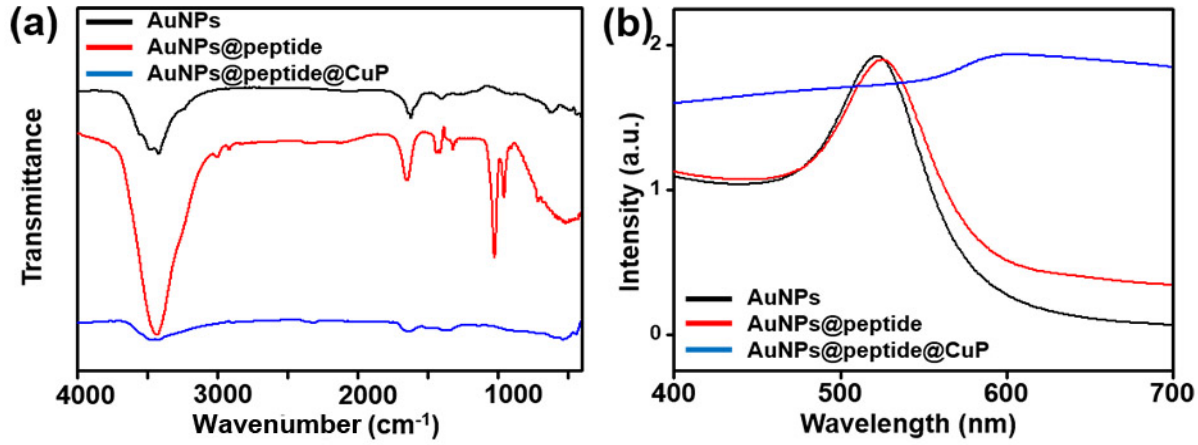

Fig. S5. (a) FT-IR spectra of AuNPs, AuNPs@BVDV peptide #2, and AuNPs@BVDV peptide #2 with CuP growth. (b) Absorption spectra of AuNPs, AuNPs@BVDV peptide #2, and AuNPs@BVDV peptide #2 with CuP growth.

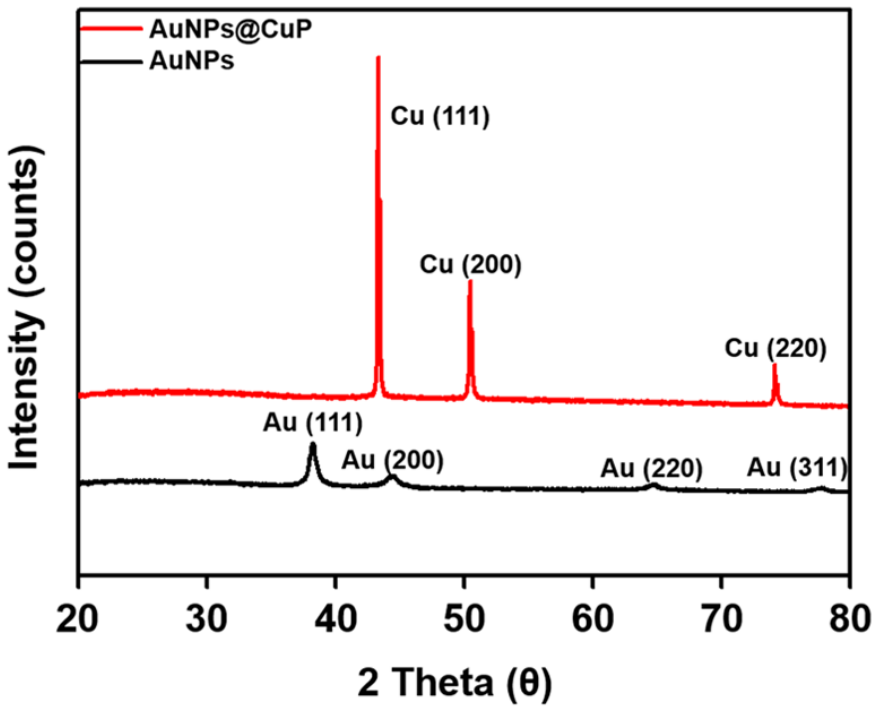

Fig. S6. X-ray diffraction patterns of AuNPs@BVDV peptide #2 and AuNPs@BVDV peptide #2@ with CuP growth.

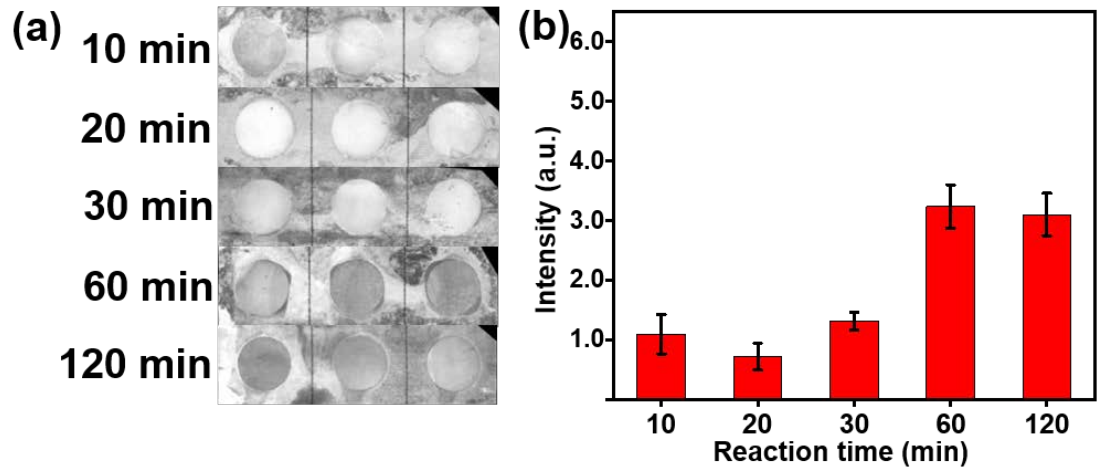

Fig. S7. (a) Smartphone camera images of dot-blot assay for the optimization of conjugation time of AuNPs@BVDV peptide #2 with BVDV (10^4 copies/mL). (b) The graph is generated between dot-blot assay intensity versus binding time (n= 3).

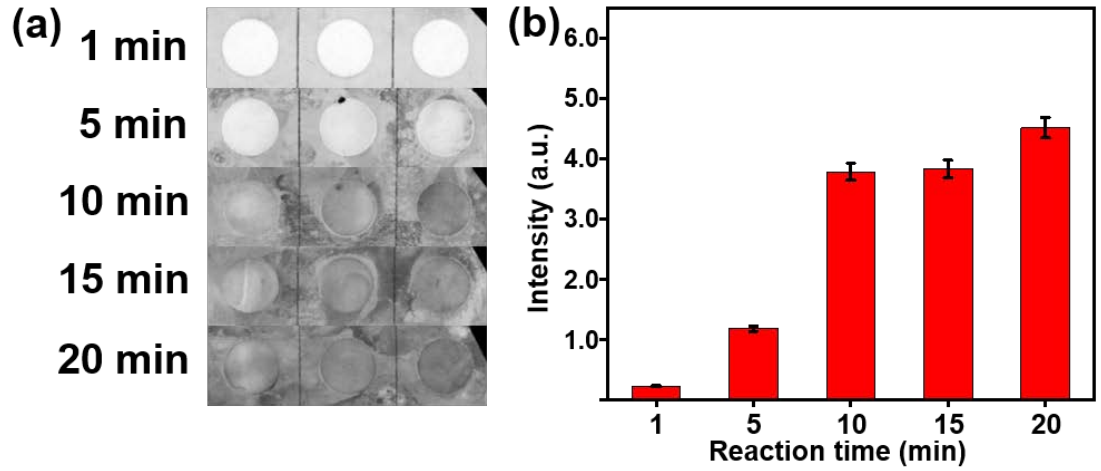

Fig. S8. (a) Smartphone camera images of dot-blot assay for the optimization of CuP growth time (1 to 20 min) using AuNPs@BVDV peptide #2 with BVDV (10^4 copies/mL). (b) The graph is generated between dot-blot assay intensity and CuP growth time (1 to 20 min) using AuNPs@BVDV peptide #2 (n= 3).

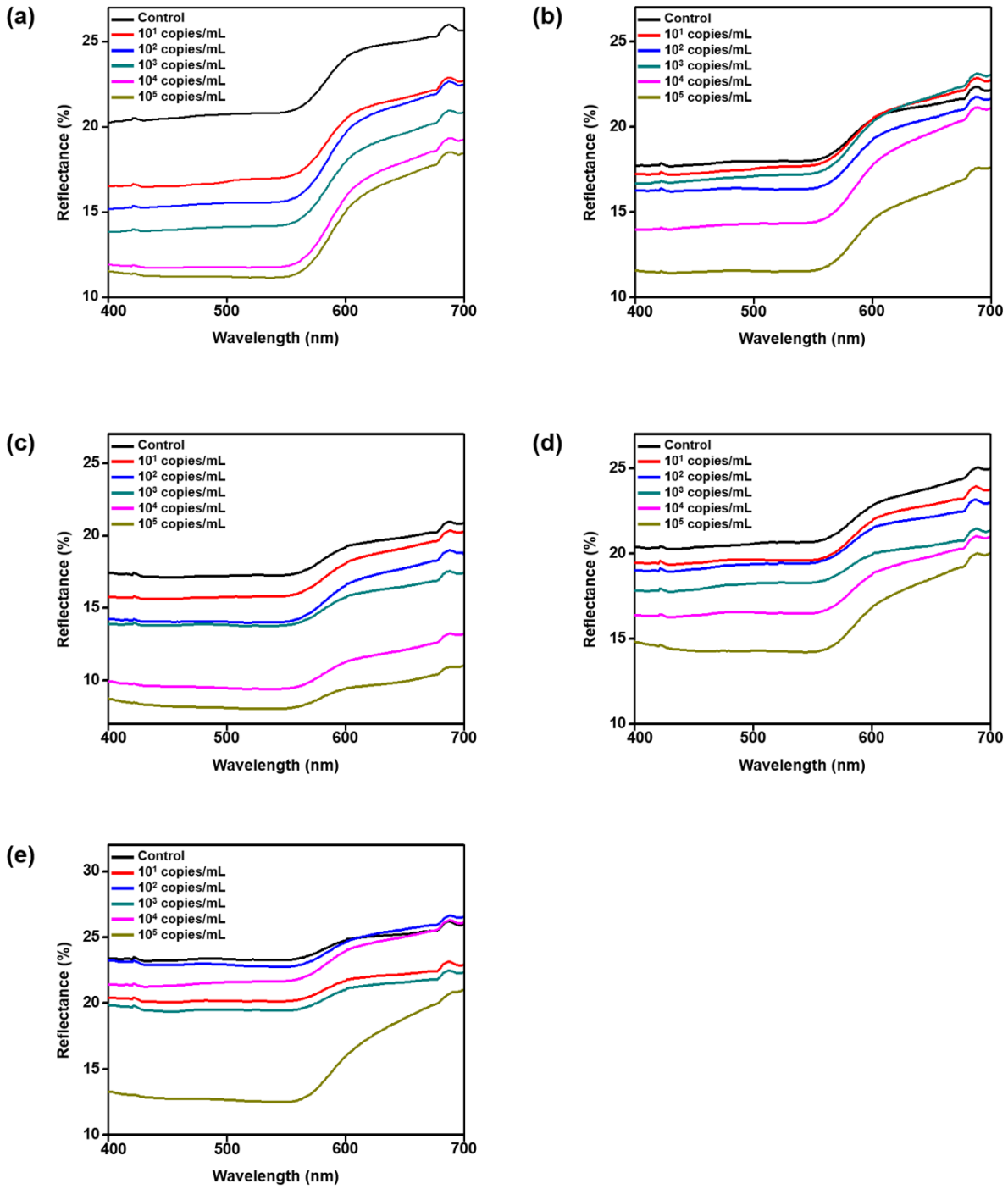

Fig. S9. UV-vis reflectance spectra of dot-blot assay with various concentrations of BVDV (0 to 10^5 copies/mL, 0 is a negative control) by using novel synthetic five candidates of BVDV affinity peptides (#2, #3, #10, #16, and #NS) conjugated to AuNPs@CuP in the presence of Cu^{2+} ion-PEI-covered growth. (a) BVDV peptide #2, (b) BVDV peptide #16, (c) BVDV peptide #3, (d) BVDV peptide #NS, (e) BVDV peptide #10 (n=3).

Table S1. The details (corresponding regression correlation coefficients) of novel synthetic affinity peptides used in this study

Name	(R^2) values	Regression curve
BVDV #2	0.9773	Y = 0.4049X + 1.527
BVDV #3	0.7751	Y = 0.3433X + 1.576
BVDV #10	0.9219	Y = 0.8801X + 1.574
BVDV #16	0.8268	Y = 0.1895X +1.089
BVDV #NS	0.4918	Y = 0.2552X + 1.090

Table S2. The summary of BVDV detection methods in previous studies

Detection method	LOD	Reaction time	Linear range	Publication Year	Reference
Microfluidic immunosensor	1.0×10^{1} $TCID_{50}$/mL	5 min	10^{1}-10^{6} $TCID_{50}$/mL	2009	[1]
Direct-charge transfer biosensor	61 CFU/mL	8 min	61-10^{2} CFU/mL	2010	[2]
SPR sensor	800 copies/mL	240 min	5.0×10^{2}-1.6×10^{4} copies/mL	2014	[3]
iiRT-PCR	23 copies/mL	65 min	23-10^{2} copies/mL	2016	[4]
ELISA and ICA with RT-PCR	1.67×10^{4} $TCID_{50}$/mL	960 min	-	2016	[5]
Light scattering methods	10^{4} MTT_{50}/mL	120 min	10^{4}-10^{7} MTT_{50}/mL	2019	[6]
Dot-blot	4.397 copies/mL	100 min	4.3 - 10^{5} copies/mL		**This study**

Additional references

1. B. C. Heinze, J.-Y. Song, C.-H. Lee, A. Najam and J.-Y. Yoon, *Sensors and Actuators B: Chemical*, 2009, **138**, 491-496.
2. Y. Luo, S. Nartker, H. Miller, D. Hochhalter, M. Wiederoder, S. Wiederoder, E. Setterington, L. T. Drzal and E. C. Alocilja, *Biosens. Bioelectron.*, 2010, **26**, 1612-1617.
3. J.-W. Park, S. J. Lee, E.-J. Choi, J. Kim, J.-Y. Song and M. B. Gu, *Biosens. Bioelectron.*, 2014, **51**, 324-329.
4. O. Lung, J. Pasick, M. Fisher, C. Buchanan, A. Erickson and A. Ambagala, *Transbound Emerg. Dis.*, 2016, **63**, e395-e402.
5. X. Zhang, T. Diraviyam, X. Li, G. Yao and A. Michael, *Biosci. Biotechnol. Biochem.*, 2016, **80**, 2467-2472.
6. X. Mi, E. M. Lucier, D. G. Turpeinen, E. L. L. Yeo, J. C. Y. Kah and C. L. Heldt, *Analyst*, 2019, **144**, 5486-5496.